

# Confounder-Dependent Bayesian Mixture Model: Characterizing Heterogeneity of Causal Effects in Air Pollution Epidemiology

Dafne Zorzetto<sup>1</sup>, Falco J. Bargagli-Stoffi<sup>2</sup>, Antonio Canale<sup>1</sup>, and Francesca Dominici<sup>2</sup>.

<sup>1</sup> Department of Statistics, University of Padova, Italy.

<sup>2</sup> Department of Biostatistics, Harvard T.H. Chan School of Public Health, Massachusetts, USA.

## Abstract

Several epidemiological studies have provided evidence that long-term exposure to fine particulate matter ( $PM_{2.5}$ ) increases mortality risk. Furthermore, some population characteristics (e.g., age, race, and socioeconomic status) might play a crucial role in understanding vulnerability to air pollution. To inform policy, it is necessary to identify mutually exclusive groups of the population that are more or less vulnerable to air pollution. In the causal inference literature, the Conditional Average Treatment Effect (CATE) is a commonly used metric designed to characterize the heterogeneity of a treatment effect based on some population characteristics. In this work, we introduce a novel modeling approach—called Confounder-Dependent Bayesian Mixture Model (CDBMM)—to characterize causal effect heterogeneity. More specifically, our method leverages the flexibility of the Dependent Dirichlet Process to model the distribution of the potential outcomes conditionally to the covariates, thus enabling us to: (i) estimate individual treatment effects, (ii) identify heterogeneous and mutually exclusive population groups defined by similar CATEs, and (iii) estimate causal effects within each of the identified groups. Through simulations, we demonstrate the effectiveness of our method in uncovering key insights about treatment effects heterogeneity. We apply our method to claims data from Medicare enrollees in Texas. We found seven mutually exclusive groups where the causal effects of  $PM_{2.5}$  on mortality are heterogeneous.

*Keywords:* Bayesian Non-parametric Modeling, Causal Inference, Dependent Dirichlet Process, Heterogeneous Causal Effects, Air Pollution Epidemiology.

# 1 Introduction

Recently, the Environmental Protection Agency (EPA) has declared the goal to “achieve environmental justice by identifying and addressing, as appropriate, disproportionately high and adverse human health or environmental effects.” More specifically, air quality regulations must take into account the unfair difference in air pollution vulnerability among people of different races, national origins, and/or social-economic statuses (U.S. Environmental Protection Agency, 2022).

Several epidemiological studies have provided evidence of adverse effects of long-term exposure to fine particulate matter ( $PM_{2.5}$ ) on human health (see, e.g., Rückerl et al., 2011; Dominici et al., 2014; Wang et al., 2016; Pope III et al., 2019; Chen and Hoek, 2020; Dominici et al., 2022). Many of these studies have relied on methods for causal inference (see, e.g., Schwartz et al., 2017; Wu et al., 2019, 2020; Lee et al., 2021). Notably, the discovery of the factors that lead to increased vulnerability to exposure to air pollution is critically important to identify vulnerable/resilient groups and, consequently, to inform the development of more effective policies. The EPA, consistently with epidemiological studies (see, e.g., Liu et al., 2021; Jbaily et al., 2022), identifies race, national origin, age, sex, and/or social-economic status as potential explanatory factors. However, to our knowledge, Bayesian data-driven methods to conduct an environmental justice analysis are underdeveloped.

Bayesian nonparametric (BNP) approaches are known for their flexibility to adapt to different contexts (Escobar and West, 1995; Green and Richardson, 2001; Hjort et al., 2010). The literature on BNP applied to causal inference, and particularly to discover factors that might lead to heterogeneity of causal effects, is quite recent (Linero and Antonelli, 2021). This literature has focused on the application or extension of the Bayesian Additive Regression Tree (BART) (Chipman et al., 2010), and dependent Dirichlet Process (DDP) mixture models (MacEachern, 2000; Barrientos et al., 2012; Quintana et al., 2020) to the causal inference framework.

The use of BART models in causal inference was first introduced by Hill (2011). Recently, Hahn et al. (2020) proposed a reparameterization of the outcome model with the inclusion of the

propensity score to control measured confounding further. Infinite mixture models have also been widely employed in causal inference literature. Notably, the Enriched Dirichlet process mixture model (Wade et al., 2011, 2014) and its modifications have found extensive and promising causal applications (Roy et al., 2018; Organisian et al., 2020a,b, 2021). For a review of BNP applications in causal inference, we refer to Linero and Antonelli (2021).

In causal inference, there is rich literature on estimating heterogeneous causal effects via the conditional average treatment effects (CATE) (see Wendling et al., 2018; Dominici et al., 2021, for a review). The CATE can be specified at different levels of *granularity*. For instance, at the highest level of granularity, one might estimate the individual treatment effect (ITE); at a lower level of granularity, one might estimate the average treatment effect for some pre-specified *groups* of the population (group average treatment effect, GATE (Jacob, 2019)). Both the ITE and GATE are special cases of CATE. Throughout, we will use CATE, rather than GATE, when referring to the estimated effects in the groups detected by the proposed algorithm.

Most of the approaches for estimating the CATE require defining covariates values (e.g. groups) *a priori*. These approaches have limitations: (i) they can be subject to the *cherry-picking* problem of reporting results only for groups with extremely high/low treatment effects (Cook et al., 2004); (ii) they must define the groups *a priori*, which in turn requires a good understanding of the treatment effects, possibly from previous literature and may fail to identify unexpected, yet important, heterogeneous groups. Despite the success in accurately estimating the CATE using machine learning methods (Hill, 2011; Hahn et al., 2020; Shin and Antonelli, 2021), the bulk of these methods offers little guidance about which groups lead to treatment effect heterogeneity. While these papers have primarily focused on the estimation of population or sample average treatment effect, few contributions have focused on the discovery and estimation of heterogeneous groups (Organisian et al., 2021; Bargagli-Stoffi et al., 2022; Lee et al., 2021, 2020).

The goal of this paper is to introduce a flexible BNP model for causal inference that can *si-*

*multaneously* (i) impute the missing potential outcomes—which in turn will allow us to estimate various causal estimands of interest defined as any functions of potential outcomes and covariates—and (ii) identify mutually exclusive groups characterizing the heterogeneity in the effects. These mutually exclusive groups are identified by different conditional treatment effects and distinguished by different values of covariates.

A nice feature of our proposed BNP model is that the estimation of the CATE within each population group does not depend on the *a priori* choice of covariates but on the groups identified by the data. Specifically, we define the distribution for the potential outcomes, conditional on the covariates and the treatment levels, as a dependent Probit Stick-Breaking Process (Rodriguez and Dunson, 2011) mixture model. In this way, we leverage information from observable characteristics to impute missing potential outcomes (Holland, 1986). Via Monte Carlo simulations, we show that, under different scenarios of the amount of heterogeneity in the causal effects, the proposed model can (i) obtain competitive results with Hill (2011)’s model—i.e. BART model for causal inference—for the estimation of individual treatment effect, and simultaneously (ii) identify mutual exclusive groups and their respective CATE, accurately. In our application, we estimate the causal effect of long-term fine particle PM<sub>2.5</sub> exposure on mortality rate for Medicare enrollees (Wu et al., 2020) in Texas. We discover seven mutually exclusive groups of Texas ZIP codes, characterized by different estimates of CATE and different social-economic and demographic features for the population.

This paper is organized as follows. In Section 2, we introduce the framework and proposed BNP model. We also develop a Gibbs sampling for sampling from the posterior distributions and estimate the model. In Section 3, we show, via Monte Carlo simulations, the ability of the proposed model to estimate the individual treatment effects to discover heterogeneous groups. Here we also compare our model’s performance with respect to the BART model. In section 4, we estimate the causal effects of the long-term fine particle PM<sub>2.5</sub> exposure and the mortality rate for Medicare enrollees (Wu et al., 2020) in Texas at the ZIP code level. In Section 5, we conclude the paper with

a discussion and avenues for future work.

## 2 Confounder-Dependent Mixture Model

### 2.1 Setup, Definitions, and Assumptions

Let  $i$  be the study unit, with  $i \in \{1, \dots, n\}$ , and  $T_i \in \{0, 1\}$  be the binary treatment with observed value  $t_i$ . According to the Rubin Causal Model Rubin (1974), the potential outcomes for unit  $i$  are defined as  $\{Y_i(0), Y_i(1)\} \in \mathbb{R}^2$ , for  $i = 1, \dots, n$ . Specifically,  $Y_i(0)$  is the outcome when the unit  $i$  is assigned to the control group, while  $Y_i(1)$  is the outcome when it is assigned to the treatment group.

In practice, however, for  $i = 1, \dots, n$ , we observe only  $y_i \in \mathbb{R}$ , that is the realization of the random variable  $Y_i$  defined as

$$Y_i := (1 - T_i) \cdot Y_i(0) + T_i \cdot Y_i(1).$$

Conversely, we can not observe the realization  $y_i^{mis} \in \mathbb{R}$  of the random variable  $Y_i^{mis}$  defined as  $Y_i^{mis} := T_i \cdot Y_i(0) + (1 - T_i) \cdot Y_i(1)$ .

Additionally, we define  $x_i$  the  $p$ -dimensional vector of subject-specific background characteristics, covariates, and potential confounders—also called pre-treatment variables. Each vector  $x_i$  can contain both categorical and continuous variables. The tuple  $(y_i, t_i, x_i)$  for  $i = 1, \dots, n$  therefore represents the observed quantities.

Our goal is to estimate the causal effect of the treatment on the outcome on the basis of the potential outcome and the observed covariates  $x$ . To do so, it is necessary to specify causal effects of interest and the assumptions needed to identify these estimands from real-world data. In particular, the causal effects are defined as functions of the two potential outcomes. While it is possible to define the causal effect in many ways, we are particularly interested in the individual causal effect

and in the conditional causal effect. Let the average treatment effect be:

$$\tau := \mathbb{E}[Y_i(1) - Y_i(0)], \quad (1)$$

where  $\tau_i = Y_i(1) - Y_i(0)$  is the individual treatment effect (ITE). Also, let the conditional average treatment effects (CATE) be

$$\tau(x) := \mathbb{E}[Y_i(1) - Y_i(0) \mid X_i = x]. \quad (2)$$

The conditional treatment effect is used to investigate and quantify the heterogeneity in the causal effects. Its estimation is useful to analyze how the effects of the treatment vary among different groups of the population.

A key goal of our proposed method is to identify the covariates  $X_i$  that play a key role in the identification of the population groups that lead to heterogeneous treatment effects.

As customary in causal inference, to identify a causal effect from the observed data, we have to make the following assumptions (Rubin, 1980).

*Assumption 1: Stable Unit Treatment Value Assumption (SUTVA).*

- (i)  $Y_i(T_i) = Y_i$ , for  $i = 1, \dots, n$ ;
- (ii)  $Y_i(T_1, T_2, \dots, T_i, \dots, T_n) = Y_i(T_i)$  for  $i = 1, \dots, n$ .

SUTVA enforces that each unit's outcome is a function of its treatment only. This is a combination of (i) consistency (no different versions of the treatment levels assigned to each unit) and (ii) no interference assumption (among the units) (Rubin, 1986).

*Assumption 2: Strong Ignorability.* Given the observed covariate vector  $x_i$ , the treatment assignment is strongly ignorable if

$$\{Y_i(1), Y_i(0)\} \perp T_i \mid X_i = x_i,$$

and  $0 < \mathbb{P}(T_i = 1 \mid X_i = x_i) < 1$ , for all  $i = 1, \dots, n$ . This assumption states that: (i) we have a random treatment assumption in each group conditional on some covariates values; (ii) all units have a positive chance of receiving the treatment.

If the SUTVA and strong the ignorability assumption hold, the estimand in (2) can be expressed as

$$\begin{aligned}\tau(x) &= \mathbb{E}[Y_i(1) \mid X_i = x] - \mathbb{E}[Y_i(0) \mid X_i = x] \\ &= \mathbb{E}[Y_i \mid X_i = x, T_i = 1] - \mathbb{E}[Y_i \mid X_i = x, T_i = 0].\end{aligned}\quad (3)$$

Notably, this framework can be easily extended to contexts where the treatment variable is a discrete variable with  $m > 2$  possible different treatments.

## 2.2 Bayesian Nonparametric Model Specification

The estimation of the causal effects can be seen as a missing data problem where, for each subject, we observe just one of the potential outcomes while the other potential outcome is always missing. Likewise, Rubin (1974) refers to the missing potential outcomes as counterfactual outcomes. From (3), we know that under strong ignorability—that is, under a sufficiently rich collection of control variables—treatment effect estimation reduces to the estimation of the conditional expectations of  $\mathbb{E}[Y_i \mid X_i = x, T_i = 1]$  and  $\mathbb{E}[Y_i \mid X_i = x, T_i = 0]$ . Provided the excellent predictive performance of Bayesian methodologies, BNP models have been widely used for this task (Sivaganesan et al., 2017; Hill, 2011; Roy et al., 2018; Hahn et al., 2020; Oganisian et al., 2021).

Here we propose a Bayesian nonparametric (BNP) approach for the conditional expectation. In particular, we exploit a dependent nonparametric mixture prior—inspired by the Dependent Dirichlet process (DDP) (MacEachern, 2000; Barrientos et al., 2012; Quintana et al., 2020). Formally, we assume for each  $i = 1, \dots, n$ :

$$\begin{aligned}\{Y_i \mid x_i, t\} &\sim f^{(t)}(\cdot \mid x_i), \\ f^{(t)}(\cdot \mid x_i) &= \int_{\Psi} \mathcal{K}(\cdot; x_i, \psi) dG_{x_i}^{(t)}(\psi), \\ G_{x_i}^{(t)} &\sim \Pi_{x_i}^{(t)},\end{aligned}\quad (4)$$

where  $\mathcal{K}(\cdot; x, \psi)$  is a continuous density function, for every  $\psi \in \Psi$ , and  $G_{x_i}^{(t)}$  is a random probability

measure depending on the confounders  $x_i$  associated to an observation assigned to treatment level  $t$ .

A priori we assume  $G_{x_i}^{(t)} \sim \Pi_{x_i}^{(t)}$  where  $\Pi_{x_i}^{(t)}$  is a treatment- and confounder-dependent nonparametric process. Following a single-atom DDP (Quintana et al., 2020) characterization of the random  $G_{x_i}^{(t)}$ , we can write:

$$G_{x_i}^{(t)} = \sum_{l \geq 1} \omega_l^{(t)}(x_i) \delta_{\psi_l^{(t)}}, \quad (5)$$

where the sequences  $\{\omega_l^{(t)}(x_i)\}_{l \geq 1}$  and  $\{\psi_l^{(t)}\}_{l \geq 1}$  represent infinite sequences of random weights and random kernel's parameters, respectively. Notably, both random sequences depend on treatment level  $t$  while the weights also depend on the confounders values  $x_i$ .

Furthermore, the sequence of dependent weights is defined through a stick-breaking representation (Sethuraman, 1994),

$$\omega_l^{(t)}(x_i) = V_l^{(t)}(x_i) \prod_{r < l} \{1 - V_r^{(t)}(x_i)\}; \quad (6)$$

where  $\{V_l^{(t)}(x)\}_{l \geq 1}$  are  $[0, 1]$ -valued independent stochastic processes. The sequence of random parameters  $\{\psi_l^{(t)}\}_{l \geq 1}$  are independent and identically distributed from a base measure  $G_0^{(t)}$ .

The discrete nature of the random probability measure  $G_{x_i}^{(t)}$  allows us to introduce the latent categorical variables  $S_i^{(t)}$  describing clusters of units defined by heterogeneous responses to the treatment level  $t$ . Assuming  $\mathbb{P}\{S_i^{(t)} = l\} = \omega_l^{(t)}(x_i)$ , we can write model in (4), exploiting conditioning on  $S_i^{(t)}$ , as

$$\{Y_i | x_i, t, \psi^{(t)}, S_i^{(t)} = l\} \sim \mathcal{K}(\cdot | x_i, \psi_l^{(t)}), \quad \psi_l^{(t)} \sim G_0^{(t)}.$$

where  $\psi^{(t)}$  represents the infinite sequence  $\{\psi_l^{(t)}\}_{l \geq 1}$ , for  $t = \{0, 1\}$ .

Among the plethora of dependent nonparametric processes (see the recent review by Quintana et al., 2020, for a detailed description), we focused on the Dependent Probit Stick-Breaking (DPSB) process for its success in applications, good theoretical properties, and ease of computation (Rodríguez and Dunson, 2011). Consistently with this, we specify:

$$V_l^{(t)}(x_i) = \Phi(\alpha_l^{(t)}(x_i)), \quad \alpha_l^{(t)}(x_i) \sim \mathcal{N}(\beta_{0l}^{(t)} + x_i^T \beta_l^{(t)}, 1), \quad (7)$$

where  $\Phi(\cdot)$  is the Probit function and  $\{\alpha_l^{(t)}(x_i)\}_{l \geq 1}$  has Gaussian distributions with mean a linear combination of the  $p$  covariates  $x_i$ .

As commonly done, we assume the kernel  $\mathcal{K}$  to be a Gaussian, so that model (4)–(5) specifies to

$$\{Y_i|x_i, t, S_i^{(t)} = l, \eta^{(t)}, \sigma^{(t)}\} \sim \mathcal{N}(\eta_l^{(t)}, \sigma_l^{2(t)}). \quad (8)$$

where  $\eta^{(t)}$  and  $\sigma^{(t)}$  represent the infinite sequences  $\{\eta_l^{(t)}\}_{l \geq 1}$  and  $\{\sigma_l^{(t)}\}_{l \geq 1}$ , respectively.

Prior elicitation is completed by assuming for the regression parameters in (7) the conjugate priors

$$\beta_{ql}^{(t)} \sim \mathcal{N}(\mu_\beta, \sigma_\beta^2),$$

for  $t = 0, 1, l \geq 1$ , and  $q = 0, 1, \dots, p$  and for the parameters  $\eta_l^{(t)}$  and  $\sigma_l^{(t)}$  in (8)

$$\eta_l^{(t)} \stackrel{iid}{\sim} \mathcal{N}(\mu_\eta, \sigma_\eta^2), \text{ and } \sigma_l^{(t)} \stackrel{iid}{\sim} \text{InvGamma}(\gamma_1, \gamma_2).$$

where  $\text{InvGamma}(\gamma_1, \gamma_2)$  represents the inverse-gamma distribution with shape parameter  $\gamma_1 \in \mathbb{R}^+$  and scale parameter  $\gamma_2 \in \mathbb{R}^+$ , and mean equal to  $\frac{\gamma_2}{\gamma_1 - 1}$  and variance  $\frac{\gamma_2^2}{(\gamma_1 - 1)^2(\gamma_1 - 2)}$ .

Sampling from the posterior distribution is straightforward via Gibbs sampling. Details are reported in the Supplementary Material.

### 2.3 Groups and Causal Effects Estimation

One of the advantages of BNP mixtures is their ability to cluster the observations. Consistently with our goal of defining heterogeneous causal effects, herein we discuss how to estimate mutually exclusive *groups* of observations, each characterized by different CATE.

Consistently with the BNP literature, we call the sets defining the estimated partition for each  $t \in \{0, 1\}$  *clusters*. We then combine these clusters to estimate the *groups* into which the observations are divided, and for each group, we calculate a different CATE. Note that we use the term *cluster* differently from *group*. The former refers to the sets defined for a specific  $t$  as a byproduct of the

infinite mixture model specification obtained through Wade and Ghahramani (2018) procedure, while the latter refers to the final groups for which we computed different CATE.

The model specification introduced in the previous section allows us to define a group of observation based on the Cartesian product of the latent categorical variables  $\{S_i^{(0)}, S_i^{(1)}\}$ , for each unit  $i = 1, \dots, n$ . Under our fully Bayesian approach, however, the couples  $\{S_i^{(0)}, S_i^{(1)}\}$  are random variables for which we can characterize the associated posterior distribution, following the computational details described in the Supplementary Material. This is customary in all Bayesian infinite mixture models, which are inherently associated with random partition models (Quintana, 2006). Under these settings, the posterior of the random partition reflects uncertainty in the clustering structure given the data (Wade and Ghahramani, 2018).

A general problem associated with the huge dimension of the space of partitions is the appropriate summarization of the posterior through a point estimate. Wade and Ghahramani (2018) propose a solution based on decision theory—i.e. the optimal point estimate is that which minimizes the posterior expectation of a loss function focusing on Binder’s loss (Binder, 1978) or Variation of Information (Meilă, 2007).

In the following analyses, we use the approach proposed by Wade and Ghahramani (2018) to divide the observations into separate clusters for each value of  $t \in \{0, 1\}$ . By using this approach, we can associate different treatments with varying numbers of clusters, which allows for a highly flexible model. For instance, in the simulations presented in Section 3, we designed Scenario 2 to have a single cluster with a constant response for the treated subjects and different clusters with varying responses depending on the confounders for the untreated group. Our proposed approach effectively accommodates such scenarios. Indeed we can reasonably imagine—i.e., in the context of exposure to air pollution—that people’s health may be affected differently in the presence of a lower level of air pollution, instead in the presence of a high level of air pollution.

Our proposed method estimates the CATE of each group without the need for a predefined

selection of a partition of the confounder space. This is achieved by directly obtaining the groups from the posterior of the model. Given that the groups are mutually exclusive, it is straightforward to identify the characteristics of the units in each group, such as the average of observed confounders or modal categories for continuous and categorical confounders, respectively.

We define the posterior distribution of the CATE for each group as the mean of the posterior distribution of the ITE for units in that group. In the following analyses, we use the mean as the posterior point estimation of CATE for each group, but other measures, such as the median, can also be used. Bayesian credible intervals for the CATE can be obtained as well. However, our proposed method allows us to define and estimate any functions of the potential outcomes conditional to the group allocation. In particular, in the application—section 4—we also estimate the Conditional Average Risk Ratio (CARR), defined as the ratio between the mean of the posterior distribution of the outcomes under exposure to high levels of air pollution and the mean of the posterior distribution of the outcomes under lower levels of air pollution, for the units allocated in each identified group.

### 3 Simulation Study

In this section, we present a simulation study to evaluate the performance of the proposed Confounder-Dependent Bayesian Mixture Model (CDBMM). Our objective is to investigate the model’s ability to (i) accurately estimate individual causal effects, (ii) correctly identify the groups of data that describe the heterogeneity in the effects, and, as a result, accurately estimate conditional treatment effects. To achieve this, we conduct simulations under four different data-generating models and analyze the results to understand the model’s behavior in different scenarios.

Specifically, in each scenario, we assume that the treatment variable and two confounders are binary and, for  $i = 1, \dots, n$  we simulate them from  $X_{1i} \sim \text{Be}(0.4)$ ,  $X_{2i} \sim \text{Be}(0.6)$ , and  $T_i \sim \text{Be}(\text{logit}(0.4X_{1i} + 0.6X_{2i}))$ , where  $\text{Be}(\theta)$  represents a Bernoulli random variable with success probability  $\theta$ . Each scenario assumes a different conformation of the groups. Each group is

obtained by introducing, for each unit, categorical variables  $S_i$  with  $k$  categories and vector of probabilities  $\boldsymbol{\pi}(X_{1i}, X_{2i})$  depending on the values of the confounders. Note that we use the words *group* and *cluster* consistently with the previous section. Conditionally on  $S_i = s$  we simulate both potential outcomes as  $Y_i(0)|S_i = s \sim \mathcal{N}(\eta_s^{(0)}, \sigma_s^{(0)})$  under control and  $Y_i(1)|S_i = s \sim \mathcal{N}(\eta_s^{(1)}, \sigma_s^{(1)})$  under treatment.

In each setting, the sample size is fixed to  $n = 800$ . For each scenario, we simulate 200 samples. In the first three scenarios we set  $k = 3$  and simulate  $S_i$  assuming  $\boldsymbol{\pi}(X_i) = (\pi_1(X_i), \pi_2(X_i))(1 - \pi_1(X_i), (1 - \pi_2(X_i))(1 - \pi_1(X_i)))$ . We define  $\pi_1(X_i) = \Phi(-1.5 + 3X_{1i})$  and  $\pi_2(X_i) = \Phi(-0.5 - 2X_{1i} + 3X_{2i})$ .

In Scenario 1, we investigate a situation in which the expected value of the outcome decreases with the treatment, but the intensity of this decrease varies across different groups. We set  $\eta^{(0)} = (2, 4, 6)$  and  $\eta^{(1)} = (0, 3, 6)$ , and assume that the variance within each group is constant, with  $\sigma_s^{(0)} = \sigma_s^{(1)} = 0.3$  for  $s = 1, 2, 3$ . This results in conditional average treatment effects of  $(-2, -1, 0)$  respectively in the three groups.

Scenario 2 examines a setting where the population has different outcomes under the control group but similar outcomes under treatment. To achieve this, we set  $\eta^{(0)} = (0, 2.2, 4.4)^T$  and  $\eta_s^{(1)} = 0$  for each  $s \in 1, 2, 3$ . Like Scenario 1, we assume that  $\sigma_s^{(0)} = \sigma_s^{(1)} = 0.3$ , resulting in conditional treatment effects of  $\tau(s) = (0, -2.2, -4.4)$  in each group.

In Scenario 3, we focus on a case where the groups are less separated, with the location parameters  $\eta^{(0)}$  and  $\eta^{(1)}$  being closer to each other and different variances between groups and for treatment and control. Specifically, we set  $\eta^{(0)} = (1, 2, 3)$ ,  $\eta^{(1)} = (0, 1.5, 3)$ ,  $\sigma^{(0)} = (0.2, 0.25, 0.25)$ , and  $\sigma^{(1)} = (0.25, 0.3, 0.2)$ . This results in conditional treatment effects of  $(-1, -0.5, 0)$ .

Finally, Scenario 4 considers a situation in which there are four groups, combining features from the previous scenarios. Specifically, we consider the values within  $\eta^{(0)}$  and  $\eta^{(1)}$  to be close to each other, as in Scenario 3, and assume different behavior under treatment and control in terms

of heterogeneity as in Scenario 2. Specifically, the outcomes under treatment show four different clusters, while the outcomes under control underline three different clusters. This is achieved by setting  $\eta^{(0)} = (1, 2, 3, 3)$ ,  $\eta^{(1)} = (0, 1.5, 3, 4.5)$ , and  $\sigma_s^{(s)} = \sigma_s^{(1)} = 0.2$  for  $s = 1, 2, 3, 4$ . The four groups are associated to the allocation probabilities  $\boldsymbol{\pi}(X_i) = (\pi_1(X_i), \pi_2(X_i)(1 - \pi_1(X_i)), \pi_3(X_i)(1 - \pi_2(X_i))(1 - \pi_1(X_i)), (1 - \pi_3(X_i))(1 - \pi_2(X_i))(1 - \pi_1(X_i)))$  where  $\pi_1 = \Phi(-0.8 - 1X_{1i} + 1X_{2i})$ ,  $\pi_2 = \Phi(0.5 - 1X_{1i} - 1X_{2i})$  and  $\phi_3 = \Phi(-1.2 - 2X_{1i} - 1X_{2i})$ . The conditional treatment effect results from  $(-1, -0.5, 0, 1.5)$  respectively in the four groups.

We choose the hyperparameters such that the prior is non-informative and in common for all the settings. For the regression parameters in (7) and for the parameters  $\eta_l^{(t)}$  and  $\sigma_l^{(t)}$  in (8) we use the following conjugate priors

$$\beta_{ql}^{(t)} \sim \mathcal{N}(0, 10), \eta_l^{(t)} \sim \mathcal{N}(0, 10), \text{ and } \sigma_l^{(t)} \sim \text{InvGamma}(5, 1).$$

for  $t \in \{0, 1\}$ ,  $l \in \{1, \dots, 20\}$ , and  $q \in \{0, 1, 2\}$ .

The performance of the proposed approach is first compared to those obtained with the Bayesian additive regression trees (BART) model by Hill (2011). We chose BART as a benchmark as this model has shown particular flexibility and an excellent performance—with the need of no or little hyper-parameter tuning—in both prediction tasks (Linero and Yang, 2018; Linero, 2018; Hernández et al., 2018) and in causal inference applications (Hill, 2011; Hahn et al., 2020; Logan et al., 2019; Nethery et al., 2019; Bargagli-Stoffi et al., 2022). Also, results from Monte Carlo simulations studies show an excellent performance of BART in causal inference settings (Dorie et al., 2019; Wendling et al., 2018).

First, we analyze the result for the average treatment effect. As illustrated in Figure 1, the results obtained from the two models are quite similar in terms of both bias and mean square error. It can be observed that the bias is close to zero, as depicted in the left plot of Figure 1, where the median of the boxplots is close to the red horizontal line that indicates a bias of zero. Additionally, the mean square errors reflect the simulated variability in each of the four scenarios.

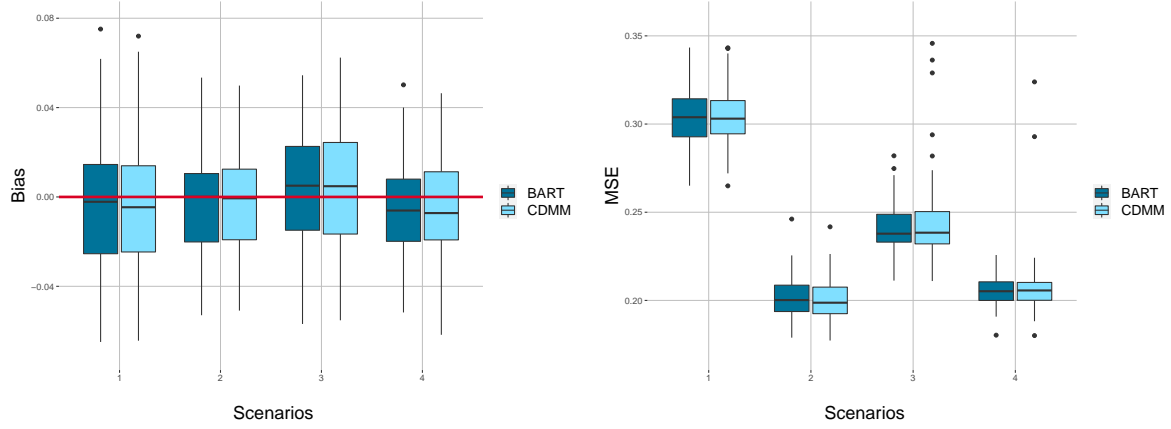


Figure 1: Comparison of estimation of individual treatment effects between CDBMM and BART: (Left) bias; (Right) mean square error.

The proposed method not only produces accurate average treatment effect estimates but also excels in estimating the conditional average treatment effect. This is evident in Figure 2, where the proposed model effectively identifies the correct number of groups in each of the four simulated scenarios. The medians of the estimated CATEs for each group are in close agreement with the true values, as evident from the close alignment with the horizontal dashed lines, demonstrating the model’s capability to distinguish between different groups and estimate the corresponding CATEs with high precision. Furthermore, our proposed method allows us to estimate several different estimands of conditional treatment effect, such as the Conditional Average Risk Ratio—whose estimates for the simulation study are reported in Section B of the Supplementary Material.

## 4 Heterogeneous Effects of Air Pollution Exposure on Mortality

The literature has found significant evidence of decreasing mortality deriving from long-term exposure to lower levels of  $\text{PM}_{2.5}$  (see Dockery et al., 1993; Beelen et al., 2014; Di et al., 2017; Liu et al., 2019; Pappin et al., 2019; Wu et al., 2020). While previous studies have made significant contributions in assessing the average treatment effect of long-term  $\text{PM}_{2.5}$ , they have primarily done

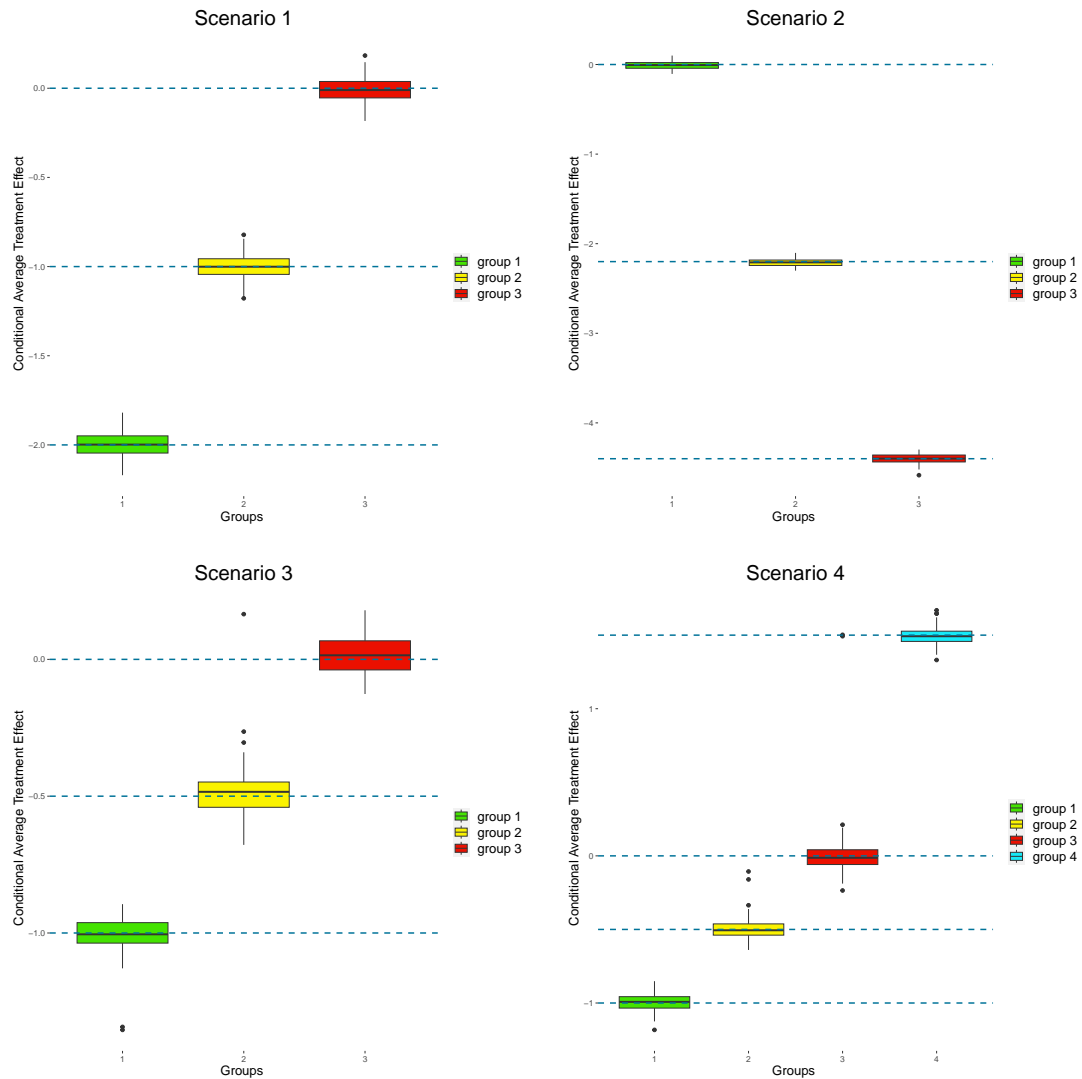


Figure 2: Conditional average treatment effect for the groups in the four simulated scenarios. The dashed lines show the true values.

so without considering potential heterogeneity in the causal effects. However, understanding how the causal effect can vary within different groups of individuals is crucial in health studies, as it can inform the development of more effective health policies.

With a focus on uncovering vulnerability/resilience in the causal effects in the context of an environmental study, we apply the proposed model to discover the heterogeneity in the health effects of exposure to higher levels of air pollution in Texas for the elderly population. Texas is a crucial case study for understanding air pollution vulnerability because of its unique demographic makeup and exposure disparities. First, recent literature has shown that, in Texas, black and low-income groups are exposed to higher levels of air pollution, whereas college graduates and high-income groups are exposed to lower levels Li et al. (2019). Second, Texas has a high proportion of Hispanic residents, which makes it a valuable case study for examining the health impacts of air pollution on this demographic group. According to the US Census Bureau, Hispanic residents make up over 39% of the Texas population (U.S. Census Bureau, 2020). Studies have shown that low-income and Hispanic communities are more likely to be exposed to higher levels of PM<sub>2.5</sub> compared to wealthier and non-Hispanic communities Jbaily et al. (2022).

Using the information on Texan Medicare enrollees (i.e., individuals older than 65) in the cohort 2010-2011, we investigate the heterogeneous causal link between long-term PM<sub>2.5</sub> exposure and mortality. Our analysis depicts how our method can discover mutually exclusive groups, estimate the heterogeneity in the effects of long-term exposure to PM<sub>2.5</sub> on the mortality rate, and identify the social-economical characteristics that distinguish the different groups.

## 4.1 Data

We conduct our analysis at the ZIP code level (1,929 units), where we have data on the following variables: the average PM<sub>2.5</sub> levels during the years 2010 and 2011; the mortality rate in the 5 follow-up years; census variables such as the percentage of residents for different races/ethnicities

(in particular, categorized as Hispanics, blacks, whites, and other races); the age of each Medicare enrollee ( $\leq 65$  years of age) and their sex (female/male); the average household income; the average home value; the proportion of residents in poverty; the proportion of residents with a high school diploma; the population density; the proportion of residents that own their house; the average body mass index; the smoking rate; the percentage of people who are eligible for Medicare (this variable is a proxy of low social-economic status and is reported as S.E.S.). Moreover, we also have access to meteorological variables: the averages of maximum daily temperatures and the relative average of humidity during summer (June to September) and winter (December to February).

The distribution of the population in Texas during 2010, how represented in the map (a) in Fig. 3, is clearly concentrated around the main cities, such as Dallas, San Antonio, Austin, and Houston, while expansive areas are quite empty, due to the desert ecosystem. Consequently, we consider only the ZIP codes with a population density different from zero and more than 10 Medicare enrollees, such that we have enough records in the Medicare dataset for that ZIP codes. For these ZIP codes, the observed values of  $PM_{2.5}$  and of mortality rates in Texas are illustrated in Figure 3—(b) and (c), respectively. Not surprisingly, the highest values on record for  $PM_{2.5}$  are primarily concentrated in the urban areas, while the mortality rate doesn't show any particular pattern.

## 4.2 Study Design

We define the treatment variable as  $T = 1$  if the average  $PM_{2.5}$  in 2010 and 2011 is above the threshold of  $10\mu g/m^3$  and  $T = 0$  otherwise. The choice of  $10\mu g/m^3$  as a threshold aligns with the new proposal for the National Ambient Air Quality Standard (NAAQS) established by the Environmental Protection Agency (EPA) (U.S. Environmental Protection Agency, 2022).

Our proposed model is applied to a matched dataset, where the census and meteorological variables are used for the matching. Matching is commonly used in observational studies to adjust for potential measured confounding bias (Rosenbaum and Rubin, 1983). In this context, similarly

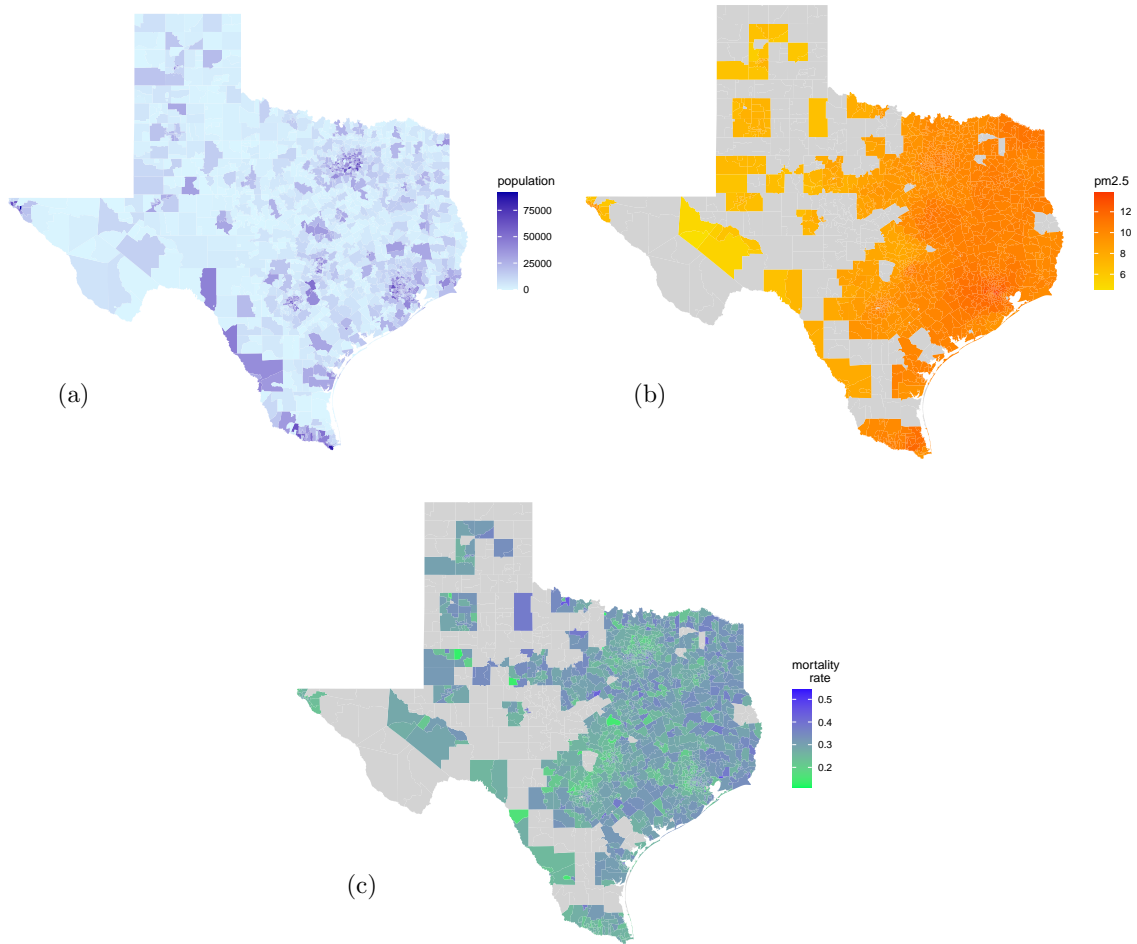


Figure 3: (a) Population density during 2010 in Texas (USA) (b) Average of long-term PM<sub>2.5</sub> exposure in 2010-2011 in Texas. The data are aggregated by ZIP codes. (c) The mortality rate at 5 follow-up years for each Texan ZIP code. The gray areas indicate the ZIP codes with population density different from zero.

to what has already been done in the literature on air pollution effects on health (see, e.g., Lee et al., 2021; Wu et al., 2020), we decide to use matching before running our model to make our analyses as robust as possible with respect to potential measured confounding bias.

We employ a 1-to-1 nearest neighbor propensity score matching, obtaining 1,402 selected units. The reduction of units is due to the different sample sizes of the treated and control groups in the original data, and 1-to-1 matching creates a sample with the same size for the treated and control groups. Using matching greatly improves the covariates balance. In Figure 4, we depict the covariate balance before and after the matching. Before the matching, there was a significant difference between the difference in standardized means of the observed values of some covariates, like poverty, education, or median household income, for the treated and control groups. These imbalances in the data might have led to spurious discoveries of effect heterogeneity. After the matching, the mean standardized differences of the covariates and the propensity score are included in the interval  $[-0.1, 0.1]$ , which is usually used as a rule-of-thumb for good quality matches (Ho et al., 2007; Austin, 2011).

### 4.3 Results

CDBMM identifies seven mutually exclusive groups in the matched ZIP codes: four where exposure to higher levels of  $\text{PM}_{2.5}$  increases the mortality rate, and three where exposure to higher levels of  $\text{PM}_{2.5}$  decreases the mortality rate. Figure 5 presents the posterior distribution of the Conditional Average Treatment Effect (CATE) and the Conditional Average Risk Ratio (CARR) for each identified group. We present results for both CATE and CARR as the information they provide is complementary, and furnishes a deeper insight into the heterogeneity in the causal effects in the case of our application. The vertical black lines in each figure represent the null causal effect, which is indicated by a CATE equal to 0 and by a CARR equal to 1.

The four groups identified by CDBMM where exposure to higher levels of  $\text{PM}_{2.5}$  increases the

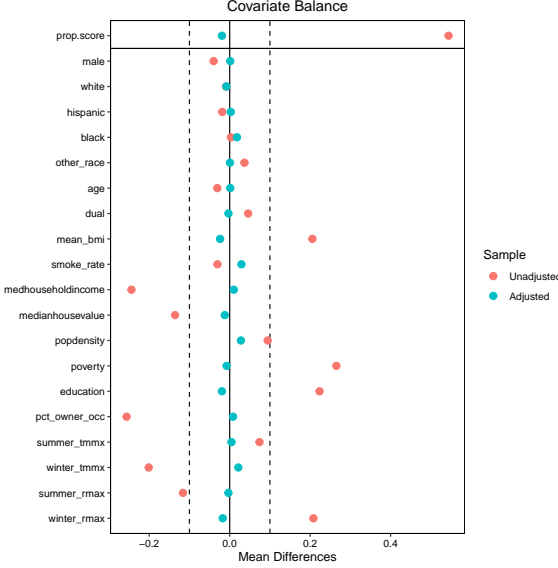


Figure 4: Comparison of the covariate balance between before and after the nearest neighbor propensity score matching 1-to-1. The continuous black vertical line indicates the value 0, while the two dotted lines are for the values  $-0.1$  and  $0.1$ , respectively.

mortality rate have positive CATE values (in order from highest to lowest: (g) 0.143, (f) 0.058, (e) 0.021, (d) 0.013) and have CARR values greater than 1 (in order: (g) 2.061, (f) 1.247, (e) 1.096, (d) 1.047). While the groups where exposure to higher levels of  $\text{PM}_{2.5}$  decreases the mortality rate have negative CATE values (in order from lowest to highest: (a) -0.017, (b) -0.021, (c) -0.104) and have CARR values less than 1 (in order: (a) 0.669, (b) 0.941, (c) 0.940).

The majority of the population (95% of ZIP codes) is included in the groups (b), (c), (d), and (e). In group (d)—including 25% of the ZIP codes—the mortality rate of the population increases by 5% under a high level of  $\text{PM}_{2.5}$ ; the bigger group (e)—including 29% of the ZIP codes—has an increment of 10% in the mortality. Conversely, the groups (b) and (c)—respectively including 24% and 17% of the ZIP codes—have a decrement of mortality by 6% under a high level of  $\text{PM}_{2.5}$ . Three small groups (a), (g), and (f) are also discovered (5% of ZIP codes). More extreme effects characterize these subgroups. An increment of up to 106% of the mortality rate when the sub-population in (g) is exposed to a high level of  $\text{PM}_{2.5}$ , and a decrement of 23% of the mortality

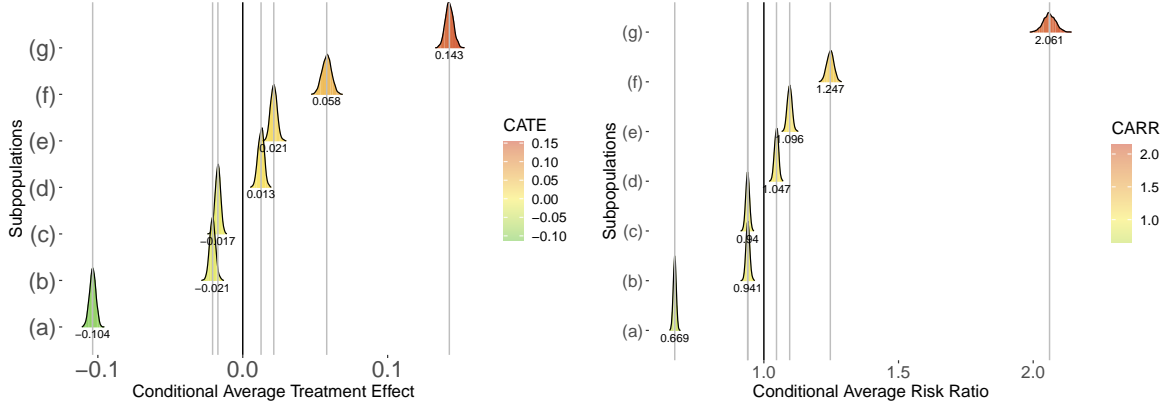


Figure 5: (Left) Posterior distribution of conditional average treatment effect (CATE) for the five discovered groups in the ZIP codes. The black line identifies the  $CATE = 0$ —i.e., the null causal effect. (Right) Posterior distribution of conditional average risk ratio (CARR) for the seven discovered groups in the ZIP codes. The black line identifies the  $CARR = 1$ —i.e., the null causal effect. In both plots, the gray lines are the mean of each posterior distribution for the CATE and the CARR, respectively.

rate when the sub-population in (a) is exposed to a high level of PM<sub>2.5</sub> instead of a lower level. These two subgroups include just 1% of the ZIP codes. Similarly, group (f)—including 2% of the ZIP codes—has a mortality rate of the population decrease by 25%. The percentages of ZIP codes allocated in the various groups are reported in Figure 6.

The demographic and socio-economic characteristics of the ZIP codes are helpful in understanding the differences in the causal effects in each identified group. The estimated model identifies mutually exclusive groups. Therefore, we can describe the distribution of these characteristics for the ZIP codes allocated in the different groups.

In the spider-plots reported in Figure 6, we can observe, for each group, the different distribution of the variables sex (close to the center indicates a bigger percentage of women in the population of the ZIP codes, far to the center a bigger percentage of men), percentage of white, Hispanic, black and other race (where smaller percentages are closer to the center), age (where the ZIP codes with age mean close to 65 years for Medicare enrollees are close to the center, and older population far from the center), and social-economic status (S.E.S.) (the center of the spider-plot indicates a

population with high income—i.e., a lower percentage of dually eligible individuals—, and far from the center lower income the opposite). Each group is identified with a different color, while the grey area reports the mean of these variables among all the analyzed ZIP codes.

Two trends characterize the groups where exposure to higher levels of  $\text{PM}_{2.5}$  increases the mortality rate. The first, composed of the groups (d) and (f), are characterized by low income, older population, and significant percentages of black and other races, respectively. These two groups identify groups of individuals for which exposure to higher levels of air pollution is highly detrimental. Consistently with the intuition, these groups are characterized by higher percentages of people from minority groups for which long-term exposure to  $\text{PM}_{2.5}$ . This could be likely due to the fact that minorities are structurally exposed to higher levels of air pollution. Exposure effects might accumulate over time—as is likely the case with  $\text{PM}_{2.5}$ —leading to increased mortality rates both for younger age (orange plot) and older age (red plot) groups (see, e.g., Pope III et al., 2019; Liu et al., 2021; Jbaily et al., 2022). The second trend —identified by groups (e) and (g)— has a population with a bigger percentage of white women, close to 65 years and high incomes, compared to the mean among all the analyzed ZIP codes. We note that this mean is the one among the ZIP codes that were introduced in our analysis after matching and might be different from the overall mean of the Texan ZIP codes.

In juxtaposition, the groups where exposure to higher levels of  $\text{PM}_{2.5}$  decreases the mortality rate are mainly composed of a population with high income characterized by black women community in group (a), old white men in group (b), and young Hispanics in group (c). This decrease in mortality when being exposed to higher levels of air pollution, while surprising, has already been documented in the literature (Liu et al., 2021; Jbaily et al., 2022). This finds an explanation in potential survival bias (see, e.g., Mayeda et al., 2018; Shaw et al., 2021). Survival bias happens in cohort studies that start later, leading to the most vulnerable individuals in certain groups dying before entering the cohort. In this case, the individuals entering the cohort are the most resilient ones and might depict

a decreasing mortality effect even when exposed to higher levels of pollutants (Liu et al., 2021).

This is likely to be the case for these three groups.

Moreover, the model identifies two distinct groups—(b) and (c)—with a similar causal effect. The importance of keeping both separated is due to the relevant difference in the two subpopulations: white old men versus young Hispanics. Indeed combining these two groups, the average of the characteristics could lead the conclusion astray.

In Section C of the Supplementary Materials, we investigate the spatial distribution of the discovered cluster in Texas.

## 5 Discussion

In this paper, we introduce a novel approach (CDBMM) for estimating average treatment effects and conditional average treatment effects under a Bayesian nonparametric framework. We find that the proposed CDBMM is a flexible approach, capable of identifying groups that drive heterogeneity of the conditional treatment effects. A key feature of the CDBMM is that the model can reliably identify the groups that lead to heterogeneity and, simultaneously, estimate the causal treatment effects within each group. In other words, under our proposed approach, we do not need to make choices *a priori* regarding which covariates could be the key drivers of heterogeneity.

In our simulation studies and real-world application, we find that CDBMM is competitive with BART in terms of estimating ITE. Additionally, CDBMM is able to correctly identify the groups and estimate the CATE with a high degree of accuracy. Our application to long-term exposure to PM<sub>2.5</sub> effects in Texas reveals seven distinct groups that characterize the heterogeneity in treatment effects. The groups identify the key factors in the population characteristics that explain different degrees of vulnerability or resilience to air pollution. In particular, we find that the groups characterized by old black/other races with low incomes or a high percentage of white young women with high incomes were found to have an increased mortality rate from exposure to PM<sub>2.5</sub>. This finding is consistent



Figure 6: Representation of the characteristics of the identified groups. Each spider plot reports in the colored area the group-specific characteristics—the mean of the analyses covariates—and in the gray area the collective characteristics—the mean of the covariates among all the analyzed Texan ZIP codes. We can consider the gray area as the benchmark to understand how the characteristics of each group differ from the collective characteristics of the analyzed Medicare enrollees in Texas.

with previous literature (see, e.g., Pope III et al., 2019; Liu et al., 2021). Conversely, for groups characterized by a high percentage of young black women, old white men, or young Hispanics, we observe a decrease in mortality which might be due to potential survival bias (Mayeda et al., 2018).

While our method is been defined for a binary treatment, it can be easily extended to handle categorical treatment as well. Similar approaches can be used in principal stratification and mediation analysis settings where one can assume the presence of a mediator/intermediate/post-treatment variable between the treatment and the outcome of interest. In such scenarios, CDBMM flexibility and performance in heterogeneous group discovery could provide an extremely valuable tool.

In conclusion, the proposed method shows promising results in the flexibility and efficiency of the nonparametric ITE and CATE estimation. In particular, the ability to identify groups defined by similar conditional treatment effects and the non-dependence of prior assumptions make the method versatile for practical applications. Furthermore, the extension to other causal inference settings paves the way for future research.

## References

Albert, J. H. and S. Chib (2001). Sequential ordinal modeling with applications to survival data. *Biometrics* 57(3), 829–836.

Austin, P. C. (2011). An introduction to propensity score methods for reducing the effects of confounding in observational studies. *Multivariate Behavioral Research* 46(3), 399–424.

Bargagli-Stoffi, F. J., K. De-Witte, and G. Gnecco (2022). Heterogeneous causal effects with imperfect compliance: a Bayesian machine learning approach. *The Annals of Applied Statistics* (3), 1986–2009.

Barrientos, A. F., A. Jara, and F. A. Quintana (2012). On the support of maceachern’s dependent Dirichlet processes and extensions. *Bayesian Analysis* 7(2), 277–310.

Beelen, R., O. Raaschou-Nielsen, M. Stafoggia, Z. J. Andersen, G. Weinmayr, B. Hoffmann, K. Wolf, E. Samoli, P. Fischer, M. Nieuwenhuijsen, et al. (2014). Effects of long-term exposure to air pollution on natural-cause mortality: an analysis of 22 European cohorts within the multicentre ESCAPE project. *The Lancet* 383(9919), 785–795.

Binder, D. A. (1978). Bayesian cluster analysis. *Biometrika* 65(1), 31–38.

Chen, J. and G. Hoek (2020). Long-term exposure to PM and all-cause and cause-specific mortality: a systematic review and meta-analysis. *Environment International* 143, 105974.

Chipman, H. A., E. I. George, and R. E. McCulloch (2010). BART: Bayesian additive regression trees. *The Annals of Applied Statistics* 4(1), 266–298.

Cook, D. I., V. J. Gebski, and A. C. Keech (2004). Subgroup analysis in clinical trials. *Medical Journal of Australia* 180(6), 289–291.

Di, Q., Y. Wang, A. Zanobetti, Y. Wang, P. Koutrakis, C. Choirat, F. Dominici, and J. D. Schwartz (2017). Air pollution and mortality in the medicare population. *New England Journal of Medicine* 376(26), 2513–2522.

Dockery, D. W., C. A. Pope, X. Xu, J. D. Spengler, J. H. Ware, M. E. Fay, B. G. Ferris Jr, and F. E. Speizer (1993). An association between air pollution and mortality in six us cities. *New England Journal of Medicine* 329(24), 1753–1759.

Dominici, F., F. J. Bargagli-Stoffi, and F. Mealli (2021). From controlled to undisciplined data: estimating causal effects in the era of data science using a potential outcome framework. *Harvard Data Science Review*.

Dominici, F., M. Greenstone, and C. R. Sunstein (2014). Particulate matter matters. *Science* 344(6181), 257–259.

Dominici, F., A. Zanobetti, J. Schwartz, D. Braun, B. Sabath, and X. Wu (2022). Assessing adverse health effects of long-term exposure to low levels of ambient air pollution: Implementation of causal inference methods. *Research Report (Health Effects Institute)* (211), 1–56.

Dorie, V., J. Hill, U. Shalit, M. Scott, and D. Cervone (2019). Automated versus do-it-yourself methods for causal inference: Lessons learned from a data analysis competition. *Statistical Science* 34(1), 43–68.

Escobar, M. D. and M. West (1995). Bayesian density estimation and inference using mixtures. *Journal of the American Statistical Association* 90(430), 577–588.

Green, P. J. and S. Richardson (2001). Modelling heterogeneity with and without the Dirichlet process. *Scandinavian Journal of Statistics* 28(2), 355–375.

Hahn, P. R., J. S. Murray, and C. M. Carvalho (2020). Bayesian regression tree models for causal inference: Regularization, confounding, and heterogeneous effects (with discussion). *Bayesian Analysis* 15(3), 965–1056.

Hernández, B., A. E. Raftery, S. R. Pennington, and A. C. Parnell (2018). Bayesian additive regression trees using Bayesian model averaging. *Statistics and Computing* 28(4), 869–890.

Hill, J. L. (2011). Bayesian nonparametric modeling for causal inference. *Journal of Computational and Graphical Statistics* 20(1), 217–240.

Hjort, N. L., C. Holmes, P. Müller, and S. G. Walker (2010). *Bayesian nonparametrics*, Volume 28. Cambridge University Press.

Ho, D. E., K. Imai, G. King, and E. A. Stuart (2007). Matching as nonparametric preprocessing for reducing model dependence in parametric causal inference. *Political Analysis* 15(3), 199–236.

Holland, P. W. (1986). Statistics and causal inference. *Journal of the American Statistical Association* 81(396), 945–960.

Jacob, D. (2019). Group average treatment effects for observational studies. *arXiv preprint arXiv:1911.02688*.

Jbaily, A., X. Zhou, J. Liu, T.-H. Lee, L. Kamareddine, S. Verguet, and F. Dominici (2022). Air pollution exposure disparities across us population and income groups. *Nature* 601(7892), 228–233.

Lee, K., F. J. Bargagli-Stoffi, and F. Dominici (2020). Causal rule ensemble: Interpretable inference of heterogeneous treatment effects. *arXiv preprint arXiv:2009.09036*.

Lee, K., D. S. Small, and F. Dominici (2021). Discovering heterogeneous exposure effects using randomization inference in air pollution studies. *Journal of the American Statistical Association* 116(534), 569–580.

Li, Z., D. M. Konisky, and N. Zirogiannis (2019). Racial, ethnic, and income disparities in air pollution: A study of excess emissions in Texas. *PLoS One* 14(8), e0220696.

Linero, A. R. (2018). Bayesian regression trees for high-dimensional prediction and variable selection. *Journal of the American Statistical Association* 113(522), 626–636.

Linero, A. R. and J. L. Antonelli (2021). The how and why of Bayesian nonparametric causal inference. *arXiv preprint arXiv:2111.03897*.

Linero, A. R. and Y. Yang (2018). Bayesian regression tree ensembles that adapt to smoothness and sparsity. *Journal of the Royal Statistical Society: Series B (Statistical Methodology)* 80(5), 1087–1110.

Liu, C., R. Chen, F. Sera, A. M. Vicedo-Cabrera, Y. Guo, S. Tong, M. S. Coelho, P. H. Saldiva, E. Lavigne, P. Matus, et al. (2019). Ambient particulate air pollution and daily mortality in 652 cities. *New England Journal of Medicine* 381(8), 705–715.

Liu, M., R. K. Saari, G. Zhou, J. Li, L. Han, and X. Liu (2021). Recent trends in premature mortality and health disparities attributable to ambient PM2.5 exposure in China: 2005–2017. *Environmental Pollution* 279, 116882.

Logan, B. R., R. Sparapani, R. E. McCulloch, and P. W. Laud (2019). Decision making and uncertainty quantification for individualized treatments using Bayesian Additive Regression Trees. *Statistical Methods in Medical Research* 28(4), 1079–1093.

MacEachern, S. N. (2000). Dependent Dirichlet processes. *Technical Report. Department of Statistics, The Ohio State University, Columbus, OH.*

Mayeda, E. R., T. J. Filshtein, Y. Tripodis, M. M. Glymour, and A. L. Gross (2018). Does selective survival before study enrolment attenuate estimated effects of education on rate of cognitive decline in older adults? A simulation approach for quantifying survival bias in life course epidemiology. *International Journal of Epidemiology* 47(5), 1507–1517.

Meilă, M. (2007). Comparing clusterings—an information based distance. *Journal of Multivariate Analysis* 98(5), 873–895.

Nethery, R. C., F. Mealli, and F. Dominici (2019). Estimating population average causal effects in the presence of non-overlap: The effect of natural gas compressor station exposure on cancer mortality. *The Annals of Applied Statistics* 13(2), 1242.

Organisian, A., N. Mitra, and J. Roy (2020a). Bayesian nonparametric cost-effectiveness analyses: Causal estimation and adaptive subgroup discovery. *arXiv preprint arXiv:2002.04706*.

Organisian, A., N. Mitra, and J. Roy (2020b). Hierarchical Bayesian bootstrap for heterogeneous treatment effect estimation. *arXiv preprint arXiv:2009.10839*.

Organisian, A., N. Mitra, and J. A. Roy (2021). A Bayesian nonparametric model for zero-inflated outcomes: Prediction, clustering, and causal estimation. *Biometrics* 77(1), 125–135.

Pappin, A. J., T. Christidis, L. L. Pinault, D. L. Crouse, J. R. Brook, A. Erickson, P. Hystad, C. Li, R. V. Martin, J. Meng, et al. (2019). Examining the shape of the association between low levels of fine particulate matter and mortality across three cycles of the canadian census health and environment cohort. *Environmental Health Perspectives* 127(10), 107008.

Pope III, C. A., J. S. Lefler, M. Ezzati, J. D. Higbee, J. D. Marshall, S.-Y. Kim, M. Bechle, K. S. Gilliat, S. E. Vernon, A. L. Robinson, et al. (2019). Mortality risk and fine particulate air pollution in a large, representative cohort of us adults. *Environmental Health Perspectives* 127(7), 077007.

Quintana, F. A. (2006). A predictive view of Bayesian clustering. *Journal of Statistical Planning and Inference* 136(8), 2407–2429.

Quintana, F. A., P. Mueller, A. Jara, and S. N. MacEachern (2020). The dependent Dirichlet process and related models. *arXiv preprint arXiv:2007.06129*.

Rodriguez, A. and D. B. Dunson (2011). Nonparametric Bayesian models through probit stick-breaking processes. *Bayesian Analysis* 6(1).

Rosenbaum, P. R. and D. B. Rubin (1983). The central role of the propensity score in observational studies for causal effects. *Biometrika* 70(1), 41–55.

Roy, J., K. J. Lum, B. Zeldow, J. D. Dworkin, V. L. Re III, and M. J. Daniels (2018). Bayesian nonparametric generative models for causal inference with missing at random covariates. *Biometrics* 74(4), 1193–1202.

Rubin, D. B. (1974). Estimating causal effects of treatments in randomized and nonrandomized studies. *Journal of Educational Psychology* 66(5), 688.

Rubin, D. B. (1980). Randomization analysis of experimental data: The fisher randomization test comment. *Journal of the American Statistical Association* 75(371), 591–593.

Rubin, D. B. (1986). Comment: Which ifs have causal answers. *Journal of the American Statistical Association* 81(396), 961–962.

Rückerl, R., A. Schneider, S. Breitner, J. Cyrys, and A. Peters (2011). Health effects of particulate air pollution: a review of epidemiological evidence. *Inhalation Toxicology* 23(10), 555–592.

Schwartz, J., M.-A. Bind, and P. Koutrakis (2017). Estimating causal effects of local air pollution on daily deaths: effect of low levels. *Environmental Health Perspectives* 125(1), 23–29.

Sethuraman, J. (1994). A constructive definition of Dirichlet priors. *Statistica Sinica*, 639–650.

Shaw, C., E. Hayes-Larson, M. M. Glymour, C. Dufouil, T. J. Hohman, R. A. Whitmer, L. C. Kobayashi, R. Brookmeyer, and E. R. Mayeda (2021). Evaluation of selective survival and sex/gender differences in dementia incidence using a simulation model. *JAMA Network Open* 4(3), e211001–e211001.

Shin, H. and J. Antonelli (2021). Improved inference for doubly robust estimators of heterogeneous treatment effects. *arXiv preprint arXiv:2111.03594*.

Sivaganesan, S., P. Müller, and B. Huang (2017). Subgroup finding via Bayesian additive regression trees. *Statistics in Medicine* 36(15), 2391–2403.

U.S. Census Bureau (2020). QuickFacts: Texas. <https://www.census.gov/quickfacts/TX>.

U.S. Environmental Protection Agency (2022). Regulatory impact analysis for the proposed reconsideration of the national ambient air quality standards for particulate matter. *Technical Report: EPA-452/P-22-001*.

Wade, S., D. B. Dunson, S. Petrone, and L. Trippa (2014). Improving prediction from Dirichlet process mixtures via enrichment. *The Journal of Machine Learning Research* 15(1), 1041–1071.

Wade, S. and Z. Ghahramani (2018). Bayesian cluster analysis: Point estimation and credible balls. *Bayesian Analysis* 13(2), 559–626.

Wade, S., S. Mongelluzzo, and S. Petrone (2011). An enriched conjugate prior for Bayesian non-parametric inference. *Bayesian Analysis* 6(3), 359–385.

Wang, Y., I. Kloog, B. A. Coull, A. Kosheleva, A. Zanobetti, and J. D. Schwartz (2016). Estimating causal effects of long-term PM2.5 exposure on mortality in New Jersey. *Environmental Health Perspectives* 124(8), 1182–1188.

Wendling, T., K. Jung, A. Callahan, A. Schuler, N. H. Shah, and B. Gallego (2018). Comparing methods for estimation of heterogeneous treatment effects using observational data from health care databases. *Statistics in Medicine* 37(23), 3309–3324.

Wu, X., D. Braun, M.-A. Kioumourtzoglou, C. Choirat, Q. Di, and F. Dominici (2019). Causal inference in the context of an error prone exposure: air pollution and mortality. *The Annals of Applied Statistics* 13(1), 520.

Wu, X., D. Braun, J. Schwartz, M. Kioumourtzoglou, and F. Dominici (2020). Evaluating the impact of long-term exposure to fine particulate matter on mortality among the elderly. *Science Advances* 6(29), eaba5692.

# SUPPLEMENTARY MATERIAL

## A Posterior Computation

Rodriguez and Dunson (2011) proves that the finite truncation of the PSB process is a good approximation; therefore, we can rewrite (5) as a finite mixture to  $L < \infty$  components with  $L$  a reasonable conservative upper bound. Rodriguez and Dunson (2011)'s proof is a key point that allows us to provide a simpler algorithm without losing the robustness of the model.

The Gibbs sampling algorithm for model fitting, which we define below, is inspired by the algorithm proposed by Rodriguez and Dunson (2011) to obtain draws from the posterior distribution. Following the steps in the algorithm 1, in each iteration  $r = 1, \dots, R$ , we use the observed data  $(y, t, x)$  to update the parameters and the augmented variables and impute the missing potential outcomes  $y^{mis}$ .

*Cluster Allocation.* The latent variables  $S_i^{(t)}$  identifies the cluster allocation for each units  $i \in \{1, \dots, n\}$  at the treatment level  $t$ . Its posterior distribution is a multinomial distribution where

$$\mathbb{P}\{S_i^{(t)} = l\} \propto \omega_l^{(t)}(x_i) \mathcal{N}(y_i; \eta_l^{(t)}, \sigma_l^{(t)2}),$$

for  $i = 1, \dots, n$  and  $l = 1, \dots, L$ , with  $\omega_l^{(t)}$  defined as:

$$\omega_l^{(t)}(x_i) = \Phi(\alpha_l^{(t)}(x_i)) \prod_{r < l} (1 - \Phi(\alpha_l^{(t)}(x_i))),$$

for  $l = 1, \dots, L - 1$  and with  $\Phi(\alpha_L^{(t)}(x_i)) = 1$ .

*Cluster Specific Parameters.* Thanks to the latent variables  $S^{(t)}$ , that cluster the units by the value of their outcome for the treatment level  $t$ , we know for each cluster  $l \in \{1, \dots, L\}$ , the allocated

units and we can update the values of the parameters from their posterior distributions:

$$\begin{aligned}\eta_1^{(t)} &\sim \mathcal{N} \left( V_1^{-1} \times \left( \frac{\sum_{\{i:S_i^{(t)}=1\}} y_i(t)}{\sigma_1^{(t)2}} + \frac{\mu_\eta}{\sigma_\eta^2} \right), V_1^{-1} \right); \\ \eta_l^{(t)} &\sim \mathcal{N} \left( V_l^{-1} \times \left( \frac{\sum_{\{i:S_i^{(t)}=l\}} y_i(t)}{\sigma_l^{(t)2}} + \frac{\mu_\eta}{\sigma_\eta^2} \right), V_l^{-1} \right) \mathbb{I}_{\{\eta_{tl} > \eta_{t(l-1)}\}}, \text{ for } l = 2, \dots, L; \\ \sigma_l^{(t)2} &\sim \text{InvGamma} \left( \gamma_1 + \frac{n_l^{(t)}}{2}, \gamma_2 + \frac{\sum_{\{i:S_i^{(t)}=l\}} (y_i(t) - \eta_l^{(t)})^2}{2} \right), \text{ for } l = 1, \dots, L;\end{aligned}$$

where  $V_l = n_l^{(t)}/\sigma_l^{(t)2} + 1/\sigma_\eta^2$ ,  $\mathbb{I}_{\{\cdot\}}$  is the indicator variable introduced in  $\eta_l^{(t)}$  distribution, to resolve the label switching problem in the MCMC chains, and  $n_l^{(t)}$  is the number of units allocated in the  $l$ -th cluster.

*Augmentation Scheme.* In order to sample from  $\{\alpha_l^{(t)}(x)\}_{l=1}^L$  and the corresponding weights  $\{\omega_l^{(t)}(x)\}_{l=1}^L$ , we need a data augmentation scheme. Its idea was developed by Albert and Chib (2001) and borrowed by Rodriguez and Dunson (2011) to obtain exact Bayesian inference for binary regression and computationally easy to include it in the Gibbs sampling (Albert and Chib, 2001). We can impute the augmented variables  $Z_l^{(t)}(x_i)$  by sampling from its full conditional distribution (Rodriguez and Dunson, 2011):

$$Z_l^{(t)}(x_i) | S_i^{(t)}, \alpha_l^{(t)}(x_i) \sim \begin{cases} \mathcal{N}(\alpha_l^{(t)}(x_i), 1) \mathbb{I}_{\mathbb{R}^+} & \text{if } S_i^{(t)} = l, \\ \mathcal{N}(\alpha_l^{(t)}(x_i), 1) \mathbb{I}_{\mathbb{R}^-} & \text{if } S_i^{(t)} < l. \end{cases}$$

The mean,  $\alpha_l^{(t)}(x_i)$ , of the previous normal distributions is obtained from:

$$\alpha_l^{(t)}(x_i) = \phi \left( \frac{\omega_{il}^{(t)}(x_i)}{\prod_{r < l} (1 - \Phi(x_i^T \beta_r^{(t)}))} \right) = \phi \left( \frac{\omega_{ir}^{(t)}(x_i)}{1 - \sum_{r < l} \omega_{ir}^{(t)}(x_i)} \right);$$

where  $\phi(\cdot)$  is the continuous density function of Gaussian distribution.

*Confounder-Dependent Weights.* To conclude the for-loop, the  $\{\beta_{ql}^{(t)}\}_{q=0}^p = (\beta_{0l}^{(t)}, \beta_l^{(t)})$ , for  $l = 1, \dots, \max(S_i^{(t)}, L - 1)$ , are updated for the posterior distribution:

$$\begin{aligned}\beta_{0l}^{(t)} &\sim \mathcal{N}((1/\sigma_\beta^2 + n)^{-1} \times (\mu_\beta/\sigma_\beta^2 + 1_n^T \tilde{\mathbf{Z}}), (1/\sigma_\beta^2 + n)^{-1}); \\ \beta_l^{(t)} &\sim \mathcal{N}_p(W^{-1} \times (\mu_\beta/\sigma_\beta^2 + (\tilde{X})^T \tilde{\mathbf{Z}}), W^{-1});\end{aligned}$$

where  $1_n$  is a  $n$  vector of ones,  $W = I_p/\sigma_\beta^2 + (\tilde{X})^T \tilde{X}$ ,  $I_p$  is a  $p \times p$  diagonal matrix,  $\tilde{X}$  is a matrix such that it is composed by the rows  $i$  in  $X$ , such that  $S_i^{(t)} \leq l$ , and  $\tilde{\mathbf{Z}}$  is a vector composed by the  $z_l^{(t)}(x_i)$  for the units  $i$  such that  $S_i^{(t)} \leq l$ .

---

**Algorithm 1** Estimation Confounder-Dependent Mixture Model (CDBMM)

---

**Inputs:** the observed data  $(y, t, x)$ .

**Outputs:**

- posterior distributions of parameters:  $\eta$ ,  $\sigma$ , and  $\beta$ ;
- posterior distribution over the space of partitions of the units.

**Procedure:**

Initialization of all parameters and latent variables.

**for**  $r \in \{1, \dots, R\}$  **do**

**for**  $t \in \{0, 1\}$  **do**

        Compute  $\omega^{(t)}(x_i)$  for  $i = 1, \dots, n$ ;

        Draw  $S_i^{(t)}$  for  $i = 1, \dots, n$ ;

        Draw  $\eta^{(t)}$  and  $\sigma^{(t)}$ ;

        Compute  $\alpha^{(t)}(x_i)$  for  $i = 1, \dots, n$ ;

        Draw  $z^{(t)}(x_i)$  for  $i = 1, \dots, n$ ;

        Draw  $\beta^{(t)}$ .

**end for**

**end for**

---

## B Estimation CARR for Simulation Study

For the four settings reported in Section 3, we have also estimated the Conditional Average Risk Ratio (CARR). CARR is defined as the ratio between the mean of the posterior distribution of the outcomes under treatment level  $t = 1$  and the mean of the posterior distribution of the outcomes under treatment level  $t = 0$  for the units allocated in each identified group.

Therefore, respectively for the four simulated settings, the CARRs are  $(0, 0.75, 1)$ ,  $(0, 0, 0)$ ,  $(0, 0.75, 1)$ , and  $(0, 0.75, 1, 1.5)$ , and their estimates are reported in Figure B.1.

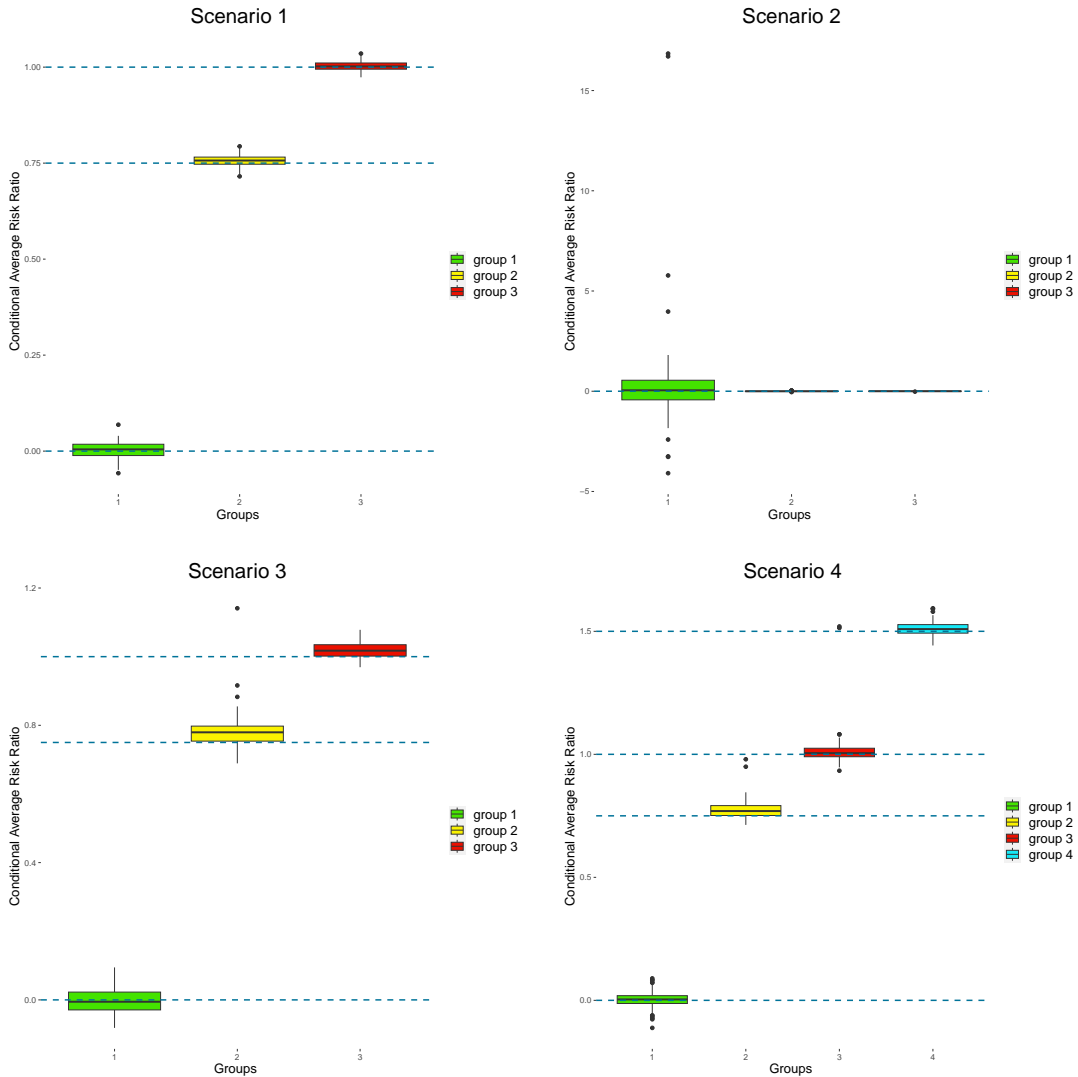


Figure B.1: Conditional Average Risk ratio (CARR) for the groups in the four simulated scenarios in Section 3. The dashed light blue lines show the true values.

## C Mapping Cluster in Texas

Here we look at the spatial distribution of the clusters identified via our CDBMM model. In particular, we find that the cluster characterized by higher vulnerability are mostly located in southern Texas. The higher-vulnerability clusters are also found in suburban areas and along interstate highways between cities. Conversely, resilient clusters can be found in more sparsely populated areas. Gray areas could not be matched and thus are excluded from our analysis.

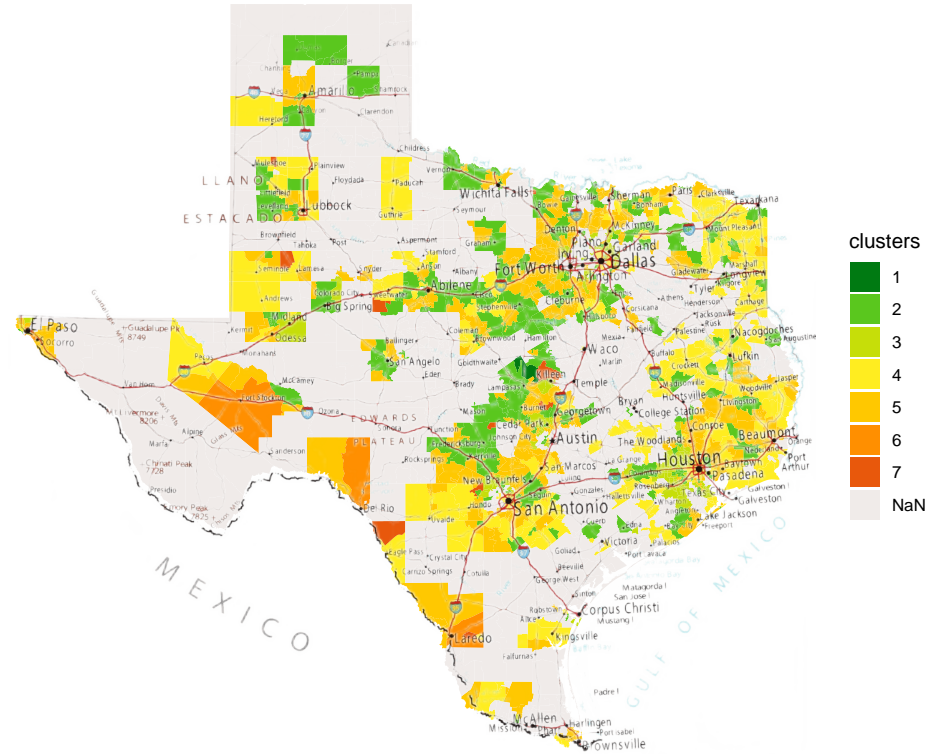


Figure C.1: Representation of the identified clusters on the map of Texas.